Inclusion of Horizontal Wind Maps in Path Planning Optimization of UAS

Anthony Reinier Hovenburg[1,2], Fabio Augusto de Alcantara Andrade[1,3,4]
Christopher Dahlin Rodin[1,2], Tor Arne Johansen[1], Rune Storvold[1,3]

***Abstract*—Earlier studies demonstrate that en-route atmospheric winds affect the in-flight performance of unmanned aircraft significantly. Nevertheless today the inclusion of wind is not common practise in determining the optimal flight path. This paper aims to contribute with an accessible method that includes forecast horizontal wind maps which are commonly available, and discuss the methods on how these maps can be integrated in order to obtain the most energy efficient horizontal path of fixed-wing aircraft. The benefits of including horizontal wind maps into the path planning optimization are demonstrated through a simulation, which utilizes Particle Swarm Optimization.**

***Index Terms*—horizontal wind, path planning, particle swarm optimization, cruise performance**

I. Introduction

Atmospheric winds pose constraints on the operations of unmanned aircraft. This holds especially true for smaller aircraft, as here it is common for wind speeds to constitute 20-50% of the airspeed [1]. This has a substantial effect on the mission safety and the aircraft's in-flight performance. It is therefore considered to be warranted to account for atmospheric winds in the planning of the aircraft's flight path. As the unmanned aircraft industry is maturing, a growing scientific search towards in-flight performance optimization is noticed. Accurate estimations of the aircraft's in-flight performance allow for optimal utilization of the system within its specified mission objectives.

Early studies demonstrate the advantages of utilizing atmospheric winds in the aircraft's route optimization [2]. More recently efforts have been made to include the complete wind field in the optimization, such as found in [3], and more recently [4], which utilize the Ordered Upwind Method and the stochastic Dijkstra algorithms, respectively, for determining the optimal flight path.

The study of path planning optimization in the context of *unmanned* aircraft is relatively new but abundant. Most notably, in [5] a method is presented that successfully incorporates wind fields in path following methods utilizing straight-line and circular arc paths. In [6] a sophisticated method was described where Model Predictive Control (MPC) methods were employed for path planning optimization, while including the effects of wind. However, neither studies included the effects of wind on the aircraft performance within the optimization, such as was the case in [4], which describes a method for the incorporation of weather uncertainty for manned aircraft in long-distance flights. In [7] the aircraft performance was successfully included, with the assumption of a constant wind field.

More recent sophisticated wind-energy harvesting methods have received increased scientific interest. Most notably in [8] two refined methods are described which utilize updraft winds from locally observed wind-fields in order to extend the aircraft's range and endurance. Considering such complex wind fields offers the potential of accurate and effective path optimization. However, the limitation of such methods in context of the study presented in this paper is that it relies on the availability of detailed local wind measurements and terrain observations or maps. In practise the extraction of lift due to *vertical* winds over terrain, known as orographic lift, is relatively complex to obtain [9]. This is in contrast to forecast horizontal wind gradients which are relatively well described, and are commonly obtainable through meteorological institutions.

The study presented in this paper positions itself in the current literature by describing an accessible method that includes forecast horizontal wind maps, and discuss the methods on how these maps can be integrated in order to obtain the most energy efficient horizontal flight path of fixed-wing unmanned aircraft. To achieve this it will specify and include the effects of horizontal winds on the in-flight performance of the aircraft. In this paper Particle Swarm Optimization technique is used, such as described in [10], in order to simulate how the inclusion wind affects the flight performance. The goal of the developed algorithm is to find the path which minimizes the total energy consumption from origin to destination by using a local wind map and by optimizing the path and airspeed of the aircraft. Minimizing the energy consumption results in a lighter aircraft as battery-powered aircraft are required to carry fewer on-board batteries, while fuel-powered aircraft require to carry less block fuel. Alternatively, one could consider the reduction in required fuel/batteries to increase the cargo capacity of the aircraft, or to offer a larger safety margin through energy reserves.

[1]NTNU Centre for Autonomous Marine Operations and System, Department of Engineering Cybernetics, Norwegian University of Science and Technology, Trondheim, Norway
[2]Maritime Robotics A/S, Trondheim, Norway
[3]NORUT Northern Research Institute, Tromsø, Norway
[4]CEFET/RJ Federal Center of Technological Education of Rio de Janeiro, Rio de Janeiro, Brazil

II. Aircraft dynamic model

The aircraft's kinematic model is described through the North-East-Down (NED) inertial reference frame. As the aim is to optimize the energy consumption per distance travelled, it is necessary to describe the wind field in a similar way. Because in this study horizontal wind maps are used, the wind field is being described in a two-dimensional plane.

When assuming a flat, non-rotating earth then x aligns north, y aligns east, and z is pointing down to earth as positive direction. Relating to the wind navigation triangle, as shown in figure 1, the aircraft's inertial velocity in a coordinated flight can be described as a function of the aircraft's ground course χ and ground speed v_g. Similarly, this can be described as a function of the true airspeed v_a, heading ψ, wind speed v_w and wind speed direction ψ_w. These relations are found through:

$$\begin{bmatrix}\dot{x}\\ \dot{y}\end{bmatrix} = v_g \begin{bmatrix}\cos\chi\\ \sin\chi\end{bmatrix} = v_a \begin{bmatrix}\cos\psi\\ \sin\psi\end{bmatrix} + v_w \begin{bmatrix}\cos\psi_w\\ \sin\psi_w\end{bmatrix} \tag{1}$$

The relation between heading and course angle is conveniently described using the law of sines, resulting in [6]:

$$\psi = \chi - \arcsin\frac{v_w}{v_a}\ \sin(\psi_w - \chi) \tag{2}$$

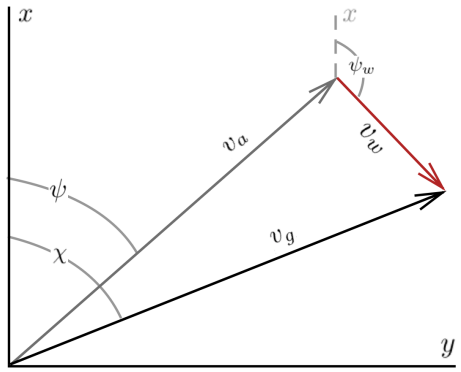

Fig. 1. Wind Navigation Triangle in Coordinated Flight

In aviation the wind maps and directional indications are often expressed in the navigation representation, rather than the mathematical representation. Therefore it is considered convenient to apply the same standards here. Here the directional indications are related to x (true north), where the clockwise rotation is positive. Note that wind maps commonly indicate the direction where the wind is coming from, rather than where it is going towards.

In an attempt to more accurately determine the aircraft's in-flight performance, one may consider including the parallel wind speed along the aircraft's heading $v_{w\psi\parallel}$. When the wind components are decomposed as demonstrated in equation (1), then the wind speed $v_{w\psi\parallel}$ can be found through:

$$v_{w\psi\parallel} = v_{wx}\ \cos\psi + v_{wy}\sin\psi \tag{3}$$

III. Effects of wind on in-flight performance

Depending on the magnitude and direction of the wind in relation to the aircraft's desired ground path, the presence of wind has an effect on the in-flight performance. In a typical mission considered in this study most in-flight time will be spend during the cruise phase. In the context of path planning optimization it is the cruise phase that is considered most relevant. The remainder of the study shall therefore consider path planning optimization methods and considerations for the cruise phase of fixed-wing unmanned aircraft.

The basis of the optimization methods presented in this paper relies on the trade-off between energy consumption and distance covered. To illustrate; when flying an A-to-B mission with a fixed distance, then the optimization goal considered in this study is to minimize the energy consumption during the execution of this mission. It is therefore required to express the aircraft's energy consumption as a function of distance covered. The power consumption (in Watts) of propeller-driven aircraft is found through [11]:

$$P_r = D\,v_a = \sqrt{\frac{2\,W^3}{\rho_\infty\,S}\frac{C_D^2}{C_L^3}} \tag{4}$$

Where W is the aircraft weight in Newtons, C_L and C_D are the aircraft's aerodynamic lift and drag coefficients respectively, ρ_∞ is the air density in kilograms per cubic meter, and S is the aircraft's effective wing surface in square meter.

The aircraft's in-flight performance can be optimized for different mission scenarios. The best range airspeed is found by flying at the airspeed where the energy consumption per travelled distance is minimized. Considering that:

$$v_a = \sqrt{\frac{2}{\rho_\infty}\left(\frac{W}{S}\right)\frac{1}{C_L}} \tag{5}$$

Then, when substituting equation (5) in (4) we find:

$$\left(\frac{P_r}{v_a}\right) = W\left(\frac{C_D}{C_L}\right) \tag{6}$$

This expression shows that the condition for maximum range occurs at the airspeed where C_L/C_D is maximized. However, as this expression relates travelled distance solely to airspeed rather than ground track speed, this does not necessarily hold true in the presence of en-route winds.

The specific energy consumption *SEC* is defined as the consumed energy per distance travelled. This can be expressed in unit Newtons, Joule per meter, or alternatively Watt-second per meter (Ws/m). Here the latter is chosen since manufacturers of battery packs often express the energy capacity in Watt-hour. By plotting the specific energy consumption (obtained from equation 6) as a function of v_w and ψ_{wr}, the complete effects of wind on the in-flight performance can be visualized. Here ψ_{wr} is the wind direction in relative to the aircraft's course.

In figure 2A such a plot is illustrated which holds valid for the aerodynamic model of the P31016 unmanned aircraft, flying at a ground velocity of 28.8 meters per second and an altitude of 1500 meters under ISA conditions. The P31016 is the unmanned platform used in the path planning scenario, which is specified further in Section IV.B.

Figure 2B shows the performance penalty of the presence of wind at the commanded ground speed of 24.0 and 28.8 meters per second, for the arbitrarily chosen ψ_{wr} of 30 degrees. This allows for the resulting air speed to be determined. This figure illustrates that for one given wind speed and direction the maximum range may be obtained by changing the commanded ground speed accordingly. Note that flying at an airspeed of 24.0 meters per second requires less power per unit *time* compared to flying at 28.8 meters per second. However, as this figure illustrates the energy consumption per unit *length* is found to be lower when flying at 28.8 meters per second. This is further demonstrated in 2C where the resulting obtainable in-flight range is illustrated for both ground speeds.

Path planning optimization algorithms that are set up so that the cost-function optimization considers the energy consumption as a function of covered ground distance in the presence of wind, will inherently optimize the commanded airspeed to give the best range. In other cases where the cost function algorithm is set up to command the desired airspeed independently of ground speed, methods such as described by [12] can be applied. In [12] it is suggested that the best-range airspeed can be approximated through:

$$m_{br} = \left[\frac{2\, m_{br} \pm \left(\frac{v_{wp}}{v_{md}}\right)}{2\, m_{br} \pm 3 \left(\frac{v_{wp}}{v_{md}}\right)} \right]^{\frac{1}{4}} \tag{7}$$

Here v_{md} is the minimum drag airspeed, v_{wp} is the wind speed along the commanded heading of the aircraft. By solving for m_{br} the ratio between the best-range airspeed in the presence of wind, and the airspeed that gives the best-range without the presence of wind can be found. The symbol $\pm$ indicates a head- or tailwind, where positive values are considered a tailwind.

Missions that requires the longest mission endurance, such as observation missions, ought to optimize the airspeed so that the energy consumption per unit time is minimized. Observing equation (4) it becomes clear that when the air density, aircraft weight, and wing surface are constant, the total energy consumption becomes a sole function of C_L and C_D. The minimum power consumption, and thus the maximum endurance, is found at the v_a where C_L^3/C_D^2 is maximized. Note that the presence of wind does not change the optimum value for v_a to achieve the maximum endurance. Similarly, path planning optimization algorithms where the cost-function considers the energy consumption as a function of time will inherently optimize the airspeed to obtain the best endurance.

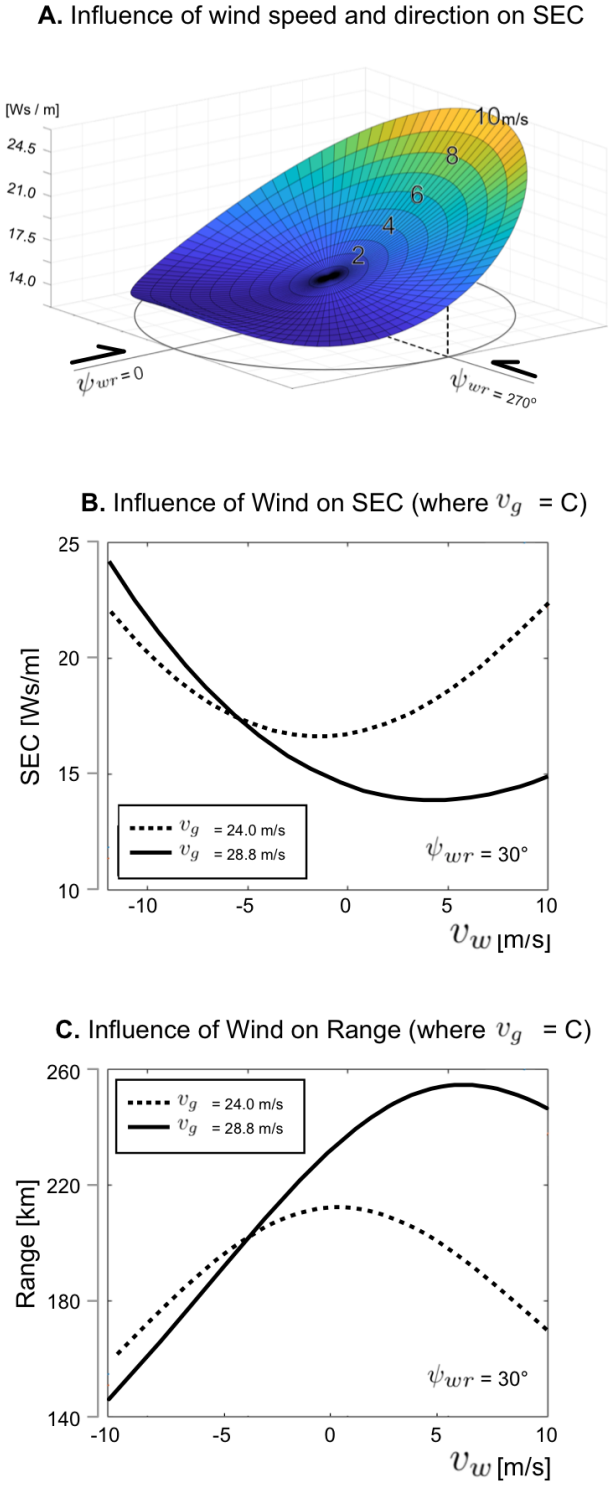

Fig. 2. A: Energy consumption of the P31016 per distance travelled as a function of wind speed, and the wind direction relative to the aircraft's course ψ_{wr}. B: SEC for different wind speed components, valid for ψ_{wr} of 30 degrees with fixed ground speeds. C: Flight range for different wind speed components, valid for ψ_{wr} of 30 degrees with fixed ground speeds.

IV. Path-Planning

In this section the path-planning solution with the inclusion of the horizontal wind maps is presented. The results are

shown after describing the optimization problem formulation, the parameters of the aircraft used for this simulation and how the wind map was obtained to perform the wind interpolation.

A. Optimization Problem Formulation

An area north of Trondheim, Norway, was chosen for this study. The objective of the optimization is to fly from A to B while using as little energy as possible, while taking the wind into consideration. To achieve this the mission waypoints and the airspeed along the path are optimized using the Particle Swarm Optimization technique, through methods as described in the Appendix.

A two-dimensional geometric approach is used in this work, where the optimization variables represent a set of airspeed inputs V and waypoints of the path W, with x (North) and y (East) positions in the NED reference frame. The altitude was chosen to be 1,500 meters.

As the positions of the origin $[x_s, y_s]$, destination $[x_t, y_t]$ and wind vectors $[v_w, \psi_w]$ are given in latitude and longitude coordinates, a conversion to the NED frame is needed. Besides, to use the result as an input for an autopilot system, it may be required to convert the waypoints to positions expressed in latitude and longitude. To reduce the error coming from the conversion between frames, the coordinates of the origin of the NED frame are defined as the midpoint between the origin and the destination.

As the path is divided into V velocity steps and W waypoints, the algorithm needs to do an interpolation to discretize the path obtained from the W waypoints into a path with V velocity steps. Therefore, the new path will have $V+1$ new interpolated waypoints, where $[x_1, y_1] = [x_s, y_s]$ will be the origin of the mission, $[x_{V+1}, y_{V+1}] = [x_t, y_t]$ will be the destination and the other $V-1$ points are resulted from the interpolation.

The cost function f is set in order to evaluate the energy consumption along the path. Therefore, it adds the energy consumption used to travel each V step through:

$$f = L_{step} \sum_{n=1}^{V} \frac{P_{r_n}}{v_{gs_n}} \tag{8}$$

where P_{r_n} is the required power (equation (4)) and v_{gs_n} is the ground speed in meters per second for the nth velocity step. L_{step} is the length of each discretized step, given by:

$$L_{step} = \frac{L}{V} \tag{9}$$

where L is the total length of the path:

$$L = \sum_{n=1}^{V} \sqrt{(x_{n+1} - x_n)^2 + (y_{n+1} - y_n)^2} \tag{10}$$

The domain (x_{min}, x_{max}, y_{min}, y_{max}) has to be defined taking into consideration that the UAS may not deviate too far from the straight line path between the origin and destination. In addition, the airspeed must be optimized within the limits of the aircraft constrains.

To initialize the optimization algorithm, first a straight path from the origin to the destination is generated - with waypoints distributed equally along the path, while the airspeed along the path is set as the airspeed that would give the best range without the presence of wind. This strategy is crucial, as usually the optimal solution will be a deviation from this straight path. If only particles initialized with random positions are used, they might have uncommon waypoints displacement, causing the algorithm to take a long time to find an optimal solution or to get stuck in a local minimum.

The other paths generated for the initialization of the optimization algorithm have the waypoints randomly chosen following the rule that the next waypoint must be closer to the destination than the previous one. The airspeed variables are randomly chosen between the minimum ($\boldsymbol{v}_{a_{min}}$) and maximum ($\boldsymbol{v}_{a_{max}}$) airspeed. Figure 3 shows an initial guess for the paths.

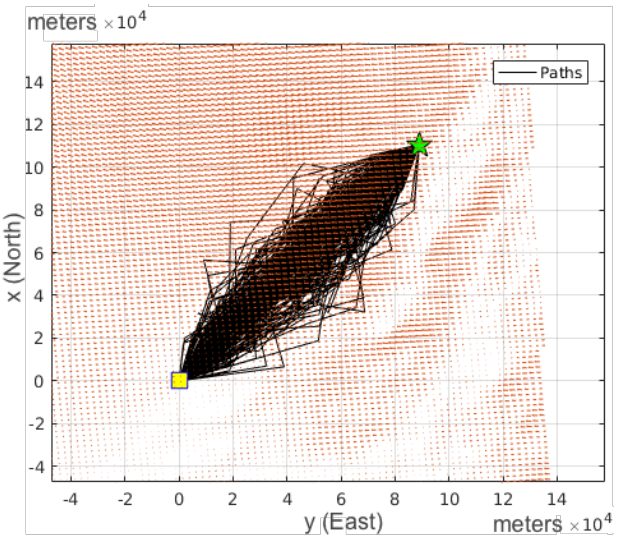

Fig. 3. 200 paths generated in the initial guess. The yellow square is the origin and the green star is the destination. The red arrows are the wind vectors.

B. Aircraft Platform

The P31016 (figure 4) is a small battery-powered aircraft that is powered by a 6.0 kilowatt brushless motor, and has a battery capacity of 977 Watt-hour. The propulsion efficiency is assumed constant at 50% with an ideal electrical discharge pattern. The aircraft has a wing surface of 0.81 square meters and has a typical mission-ready mass of 17.5 kilograms. Its aerodynamic characteristics were determined through a simplified model of the aircraft in the software tool XFLR5. Here it was found that at an altitude of 1,500 meters under ISA conditions the airspeed for maximum range occurs at 28.8 meters per second, while the airspeed for maximum endurance is found at 24.0 meters per second. The aircraft's stall speed with extended flaps is 12 meters per second, while the maximum speed is limited to 38 meters per second.

Fig. 4. P31016 concept battery-powered fixed-wing unmanned aircraft

C. Wind vector maps

The horizontal wind map used were originally obtained from the Norwegian Meteorological Institute (MET), and provided by the Norwegian Defence Research Establishment (FFI). The wind map contains the amplitude and direction of the wind for each point in the grid at a given altitude. The grid has a resolution of approximately 2.5 kilometers, and the position of the points are given as the latitude and the longitude. Figure 5 illustrates a section of the wind map used.

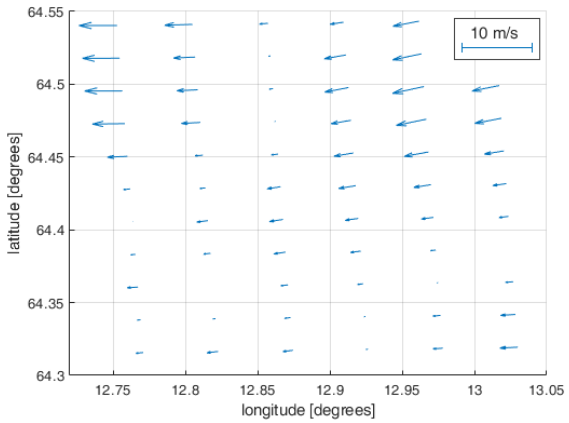

Fig. 5. Part of the wind map used. The arrows show the amplitude and direction of the wind for each point in the grid.

In order to obtain wind data in between the grid points in the wind map, the wind data needs to be interpolated. Nearest neighbor interpolation could be used for fast interpolation, and could provide sufficient accuracy for a smooth wind field. However, the discontinuity of nearest neighbor interpolation or abrupt wind changes could cause significant errors. In order to improve this, biharmonic spline interpolation [13] is used. Biharmonic spline interpolation has the benefits of creating a smooth surface (has minimum curvature) and passes through each data point. To obtain a sufficiently low computation time, the 16 surrounding grid points (the smallest and second smallest squares, each containing unique grid points, and enclosing the point to be interpolated) are selected as the data points for calculating the interpolation function.

D. Results

The parameters chosen to set the optimization algorithm are shown in Table I. Figure 6 shows the optimized path (black dots) for the mission where the objective is to fly from the yellow square (origin) to the green star (destination). The algorithm has optimized the position of the five waypoints (blue dots) and the airspeed at each V-step. The resulted optimized airspeed is shown in figure 7. In this mission the total energy consumption calculated for the straight line path, when flying at the no-wind best-range airspeed of 28.8 meters per second, was 691 Watt-hour. The total energy consumption of the optimized path was 662 Watt-hour. This is a saving of 4.2% of consumed energy. This is despite the fact that the optimized path is 3.6 kilometers longer than the straight path. An overview of the results of the flight time, path length and energy consumption as a comparison between the straight path and the optimized path are shown in Table II.

TABLE I
LIST OF PARAMETERS

Name	Value
Iterations	200
Particles	200
Waypoints (W)	5
V	50
Particle Size	55
Particle velocity constraint	0.1 x Domain
w_{ini}	1.0
w_{fin}	0.1
x_{min}	x_s-$L_{min}/3$
x_{max}	x_t+$L_{min}/3$
y_{min}	y_s-$L_{min}/3$
y_{max}	y_t+$L_{min}/3$
$v_{a_{min}}$	18 m/s
$v_{a_{max}}$	38 m/s

TABLE II
SIMULATION RESULTS

	Straight Path	Optimized Path
Length	141.8 km	145.4 km
Time	1h 37min	1h 29min
Consumed energy	691 Wh	662 Wh

V. DISCUSSION AND FUTURE WORK

The wind maps used in this study represents the wind information obtained through meteorological wind models. As the current wind map is only valid for that moment in time, for longer flights it may prove useful to include forecast wind maps valid for future time windows. Moreover, in-situ path planning may be complemented with real-time wind field estimations through methods such as described in [8]

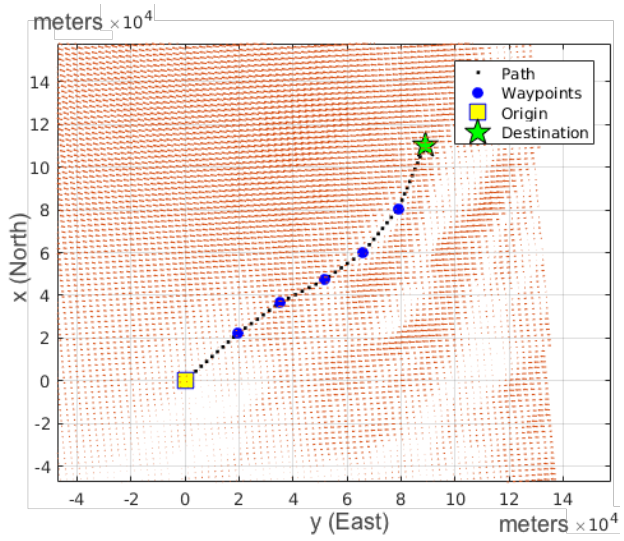

Fig. 6. Final path - Accounting for en-route winds

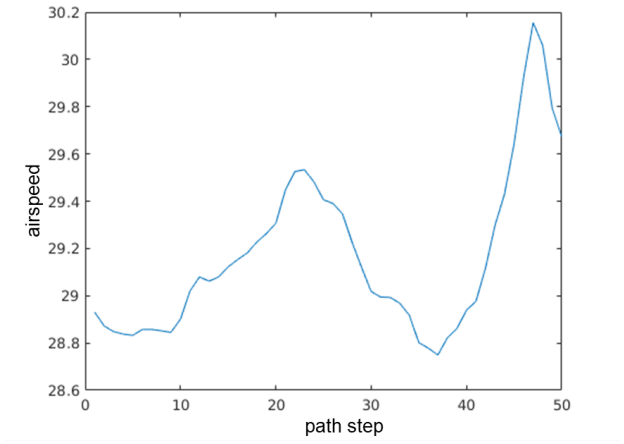

Fig. 7. Optimized commanded airspeed along the route

and [14]. In the submitted work described in [15] a real-time field estimation method is described utilizing a moving horizon estimator, which may be used to identify both steady and turbulent wind velocities.

The simulation results presented in this paper are valid for one chosen scenario. Depending on the local wind field and aerodynamic characteristics of the aircraft the obtainable savings may be higher or lower for other scenarios. The authors consider it to be warranted to extend this research in the future with more varied scenarios, while having a validated aerodynamic model and propulsion efficiency model of the used aircraft. Finally, the accuracy of the simulation results are as always limited by the accuracy of the input parameters, which to a large extend include the predicted wind field model. As horizontal wind maps do not specify vertical wind components, these effects are not included. It is therefore warranted that in a future research the proposed model is verified through field tests. This is done preferably for a variety of mission scenarios with a different wind field, altitude and terrain.

In a future work the authors intend to complement the proposed method with the ability to include horizontal wind maps of different altitudes, and thereby effectively creating a quasi-three-dimensional wind field. This allows for en-route adjustment of the cruise altitude which has the potential to further increase the obtained flight efficiency.

VI. Conclusion

In this study a method was presented for the inclusion of horizontal wind maps into a path planning optimization algorithm. An aircraft performance model is presented that incorporates the effects of wind on the in-flight energy consumption, in relation to the airspeed and the resulting ground speed. It is demonstrated that in the presence of wind the best-range airspeed is no longer found at the airspeed associated with $(C_L/C_D)_{max}$, thus en-route airspeed optimization is warranted. It is described that when the goal is to maximize the flight range, an optimization algorithm which is set up to optimize the commanded airspeed in order to minimize the energy consumption as a function of ground distance covered, will inherently command the optimal course and airspeed in the presence of wind.

A simulation was performed where a particle swarm optimization method was utilized to determine the wind-optimized flight path, where an in-situ forecast 2D wind field was incorporated. The performed simulation shows that when comparing the wind-optimized flight path to the straight path, the length increased with 3.6 kilometers to a total of 145.4 kilometers. However, the flight time was reduced by eight minutes and the total consumed energy was reduced by 4.2%. These simulation results are valid for the chosen scenario utilizing the P31016 unmanned aircraft. In future work it should be particularly interesting to simulate a more diverse wind field. In addition it is warranted to validate the proposed model through field experiments.

Acknowledgement

The authors want to thank Morten Hansbø at the Norwegian Defence Research Establishment (FFI) for supplying the local wind models that were used in this study.

This work has been carried out at the Centre for Autonomous Marine Operations and Systems (AMOS), supported by the Research Council of Norway through the Centres of Excellence funding scheme, project number 223254. This project has received funding from the European Union's Horizon 2020 research and innovation programme under the Marie Sklodowska-Curie grant agreement No 642153.

Appendix
Particle Swarm Optimization

Particle Swarm Optimization (PSO) [10] is a technique that uses a population of solutions that explores the hyperspace of a problem at a defined speed, which is adjusted according to

the best individual historical solution p_{best}, and with the best historical global solution g_{best}. This evaluation is performed by calculating the cost function (equation 8). Calculating the cost function according to the position of the particle makes it possible to identify whether the new position is better than that previously occupied by the particle. Thus, at each iteration a new velocity, i.e., the movement in the domain space, is adjusted as a function of p_{best} and g_{best}. This is done so that each particle explores the hyperspace optimally, as it takes into consideration the historical performance of the population. This procedure is illustrated in figure 8. Through this method the movement of each particle is considered to naturally evolve into the optimal (solution) position.

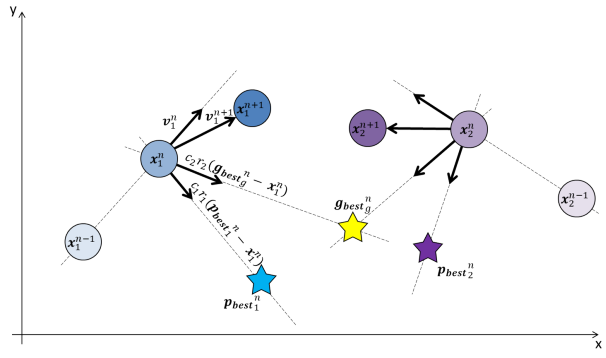

Fig. 8. Behavior of two particles in an arbitrary two-dimensional space

This technique is notable for its simplicity as the behavior of each particle, and therefore the set of presumed solutions, is defined by only two iterative equations. These determine the position x_i^n and velocity v_i^n of the particle i at time n, resulting in:

$$v_i^{(n+1)} = v_i^n + c_1\, r_1({p_{best_i}}^n - x_i^n) + c_2\, r_2({g_{best_g}}^n - x_i^n) \tag{11}$$

$$x_i^{(n+1)} = x_i^n + v_i^{(n+1)} \tag{12}$$

where c_1 and c_2 are called acceleration coefficients, which are related to the local and global portion, respectively; and with r_1 and r_2 representing the stochastic factor of these accelerations. These are usually chosen as a uniformly distributed random value between 0 and 1.

The PSO algorithm corresponds to the pseudocode shown in Algorithm 1:

Several authors proposed modifications to the basic algorithm. In this study two small modifications proposed by the original creators of the algorithm are adopted; position and velocity boundary constraints as described in [16], and linear inertia weight as described in [17].

The PSO algorithm evolves by updating the particle position for each iteration in relation to the velocity vector. Such updates have stochastic gains, where it is undesirable that the particles move uncontrollably. A particle that has a high velocity in relation to the total domain size, may eventually

Algorithm 1 PSO

```
Initialize a swarm with random positions and velocities
while Stop criteria is not satisfied do
    for Each particle i do
        Calculate the new velocity
        Update the position
        Evaluate the cost function f(x_i)
        if f(x_i) < f(p_best_i) then
            p_best_i ← x_i
        end if
        if f(x_i) < f(g_best_g) then
            g_best_g ← x_i
        end if
    end for
end while
```

jump to a distant point inside the domain. This results in the particle no longer performing a minutely search for the optimum. To avoid this problem, the concept of position and velocity constraints was developed.

Another fundamental strategy is to limit the search domain in relation to the optimization problem in question. To prevent the particle from exploring distant regions away from the region that has the optimal solution, or to prevent from bringing solutions outside the problem domain.

Here the basic idea is to avoid for the particle to leave the domain where the optimal solution resides.

The constraints can be implemented through:

$$v_i = \begin{cases} V_{max} & \text{if } v_i > V_{max} \\ -V_{max} & \text{if } v_i < -V_{max} \\ v_i & \text{otherwise} \end{cases} \tag{13}$$

The following conditions are added to the algorithm:

$$x_i = \begin{cases} X_{max} & \text{if } x_i > X_{max} \\ X_{min} & \text{if } x_i < X_{min} \\ x_i & \text{otherwise} \end{cases} \tag{14}$$

The final modification is to permit a better control of the search domain. The inertia weight, indicated in the following equation as w^n, is applied to the current velocity v_i^n, during the process of calculating the new velocity of the particle:

$$v_i^{(n+1)} = w^n v_i^n + c_1\, r_1({p_{best_i}}^n - x_i^n) + c_2\, r_2({g_{best_g}}^n - x_i^n) \tag{15}$$

When a constant value is chosen for the inertia weight, high values imply high velocities, which can make the particle to traverse the entire search domain more quickly; while low values slow down, limiting the search domain of the particle to its neighborhood. Initially, a constant value was proposed for the inertia weight. However, proposals of dynamic values that varied linearly appeared later.

In this specific case the consensus is that initially it is more convenient for the particle to have a global search power,

and only afterwards perform a more local exploration. In the linear inertia weight, if N is the maximum number of iterations, nd w_{ini} and w_{fin} are the values of the initial and final inertia weight, the inertia weight for the iteration n is determined by:

$$w^n = (w_{ini} - w_{fin})\frac{(N-n)}{N} + w_{fin} \tag{16}$$

REFERENCES

[1] R. Beard and T. McLain, *Small Unmanned Aircraft: Theory and Practice*. Princeton University Press, 2012.

[2] A. Chakravarty, "Four-dimensional fuel-optimal guidance in the presence of winds," *Journal of Guidance*, vol. 8, pp. 16–22, 1985.

[3] B. Girardet, L. Lapasset, D. Delahaye, and C. Rabut, "Wind-optimal path planning: Application to aircraft trajectories," *13th International Conference on Control Automation Robotics and Vision, ICARCV 2014*, pp. 1403–1408, 2014.

[4] A. Franco, D. Rivas, and A. Valenzuela, "Optimal aircraft path planning considering wind uncertainty," *European Conference for aeronautics and Space Sciences (EUCASS)*, 2017.

[5] D. R. Nelson, D. B. Barber, T. W. Mclain, and R. W. Beard, "Vector field path following for miniature air vehicles," *IEEE Transactions on Robotics*, vol. 23, pp. 519–529, 2007.

[6] A. Rucco, A. P. Aguiar, and F. L. Pereira, "A predictive path-following approach for fixed-wing unmanned aerial vehicles in presence of wind disturbances," *Robot 2015: Second Iberian Robotics Conference*, vol. 8, pp. 623–634, 2016.

[7] M. Coombes, W.-H. Chen, and P. Render, "Landing site reachability in a forced landing of unmanned aircraft in wind," *Journal of Aircraft*, vol. 54, pp. 1415–1427, 2017.

[8] S. Gudmundsson, V. Golubev, S. Drakunov, and C. Reinholtz, "Biomimemic opportunistic approaches in energy-conserving/harvesting flight-path modeling for uas," *AIAA Modeling and Simulation Technologies Conference*, 2016.

[9] M. J. Mears, "Energy harvesting for unmanned air vehicle systems using dynamic soaring," *50th AIAA Aerospace Sciences Meeting Including the New Horizons Forum and Aerospace Exposition*, January 2012.

[10] R. Eberhart and J. Kennedy, "A new optimizer using particle swarm theory," in *Micro Machine and Human Science, 1995. MHS'95., Proceedings of the Sixth International Symposium on*. IEEE, 1995, pp. 39–43.

[11] J. Anderson, *Aircraft performance and design*, ser. McGraw-Hill international editions: Aerospace science/technology series. WCB/McGraw-Hill, 1999.

[12] F. J. Hale and A. R. Steiger, "Effects of wind on aircraft cruise performance," in *1978 AIAA Aircraft Systems and Technology Conference*. American Institute of Aeronautics and Astronautics, Aug. 1978.

[13] D. T. Sandwell, "Biharmonic spline interpolation of geos-3 and seasat altimeter data," *Geophysical Research Letters*, vol. 14, no. 2, pp. 139–142, 1987.

[14] J. W. Langelaan, N. Alley, and J. Neidhoefer, "Wind field estimation for small unmanned aerial vehicles," *Journal of Guidance, Control, and Dynamics*, vol. 34, no. 4, pp. 1016–1030, 2011.

[15] S. Benders, A. W. Wenz, and T. A. Johansen, "Adaptive path planning for unmanned aircraft using in-flight wind estimation," *Submitted to 2018 International Conference on Unmanned Aerial Systems*, 2018.

[16] R. C. Eberhart, Y. Shi, and J. Kennedy, *Swarm intelligence*. Elsevier, 2001.

[17] R. C. Eberhart and Y. Shi, "Comparing inertia weights and constriction factors in particle swarm optimization," in *Evolutionary Computation, 2000. Proceedings of the 2000 Congress on*, vol. 1. IEEE, 2000, pp. 84–88.